Klickstein, L. B., Wong, W. W., Smith, J. A., Weis, J. H., Wilson, J. G., & Fearon, D. T. (1987) *J. Exp. Med. 165*, 1095-1112.
Klickstein, L. B., Bartow, T. J., Miletic, V., Rabson, L. D., Smith, J. A., & Fearon, D. T. (1988) *J. Exp. Med. 168*, 1699-1717.
Koistinen, V., Wessberg, S., & Leikola, J. (1989) *Complement Inflammation 6*, 270-280.
Kristensen, T., Wetsel, R. A., & Tack, B. F. (1986) *J. Immunol. 136*, 3407-3411.
Laemmli, U. K. (1970) *Nature 227*, 680-685.
Lambris, J. D. (1988) *Immunol. Today 9*, 387-393.
Lambris, J. D., & Ross, G. D. (1982) *J. Exp. Med. 155*, 1400-1411.
Lambris, J. D., & Müller-Eberhard, H. J. (1984) *J. Biol. Chem. 259*, 12685-12690.
Lambris, J. D., Dobson, N. J., & Ross, G. D. (1980) *J. Exp. Med. 152*, 1625-1644.
Lambris, J. D., Avila, D., Becherer, J. D., & Müller-Eberhard, H. J. (1988) *J. Biol. Chem. 263*, 12147-12150.
Lambris, J. D., Ganu, V. S., Hirani, S., & Müller-Eberhard, H. J. (1985) *Proc. Natl. Acad. Sci. U.S.A. 82*, 4235-4239.
Lublin, D. M., Liszewski, M. K., Post, T. W., Arce, M. A., LeBeau, M. M., Rebentisch, M. B., Lemons, R. S., Seya, T., & Atkinson, J. P. (1988) *J. Exp. Med. 168*, 181-194.
Matsudaira, P. (1987) *J. Biol. Chem. 262*, 10035-10038.
Medof, M. E., Lublin, D. M., Holers, V. M., Ayers, D. J., Getty, R. R., Leykam, J. F., Atkinson, J. P., & Tykocinski, M. L. (1987) *Proc. Natl. Acad. Sci. U.S.A. 84*, 2007-2011.
Merrifield, R. B. (1963) *J. Am. Chem. Soc. 85*, 2149.
Moore, M. D., Cooper, N. R., Tack, B. F., & Nemerow, G. N. (1987) *Proc. Natl. Acad. Sci. U.S.A. 84*, 9194-9198.
Morley, B. J., & Campbell, R. D. (1984) *EMBO J. 3*, 153-157.
Nilsson, B., & Nilsson, U. R. (1987) *J. Immunol. 138*, 1858-1863.
Pangburn, M. K. (1986) *J. Immunol. 136*, 2216-2221.
Pangburn, M. K., & Müller-Eberhard, H. J. (1978) *Proc. Natl. Acad. Sci. U.S.A. 75*, 2416-2420.
Pryzdial, E. L. G., & Isenman, D. E. (1987) *J. Biol. Chem. 262*, 1519-1525.
Reid, K. B. M., Bentley, D. R., Campbell, R. D., Chung, L. P., Sim, R. B., Kristensen, T., & Tack, B. F. (1986) *Immunol. Today 7*, 230-234.
Ripoche, J., Day, A. J., Harris, T. J. R., & Sim, R. B. (1988) *Biochem. J. 249*, 593-602.
Ross, G. D., Lambris, J. D., Cain, J. A., & Newman, S. L. (1982) *J. Immunol. 129*, 2051-2060.
Stewart, J. C., Pensa, C., Matsueda, G., & Harris, K. (1976) in *Peptides* (Loffer, A., Ed.) pp 285-290, Editions de l'-Universitê de Bruxelles, Bruxelles.
Tamerius, J. D., Pangburn, M. K., & Müller-Eberhard H. J. (1982) *J. Immunol. 128*, 512-514.
Towbin, H., Staehelin, T., & Gordon, J. (1979) *Proc. Natl. Acad. Sci. U.S.A. 76*, 4350-4354.
Ueda, A., Kearney, J. F., Roux, K. H., & Volanakis, J. E. (1987) *J. Immunol. 138*, 1143-1149.
Weis, J. J., Fearon, D. T., Klickstein, L. B., Wong, W. W., Richards, S. A., de Bruyn Kops, A., Smith, J. A., & Weis, J. H. (1986) *Proc. Natl. Acad. Sci. U.S.A. 83*, 5639-5643.

Role of Hydrophobic Forces in Bilayer Adhesion and Fusion†

Christiane A. Helm,‡ Jacob N. Israelachvili,*,§ and Patty M. McGuiggan§

Institut für Physikalische Chemie, Johannes Gutenberg-Universität, Jakob-Welder Weg 11, D-6500 Mainz, Germany (FRG), and Department of Chemical and Nuclear Engineering and Materials Department, University of California, Santa Barbara, California 93106

Received March 25, 1991; Revised Manuscript Received November 13, 1991

ABSTRACT: With the aim of gaining more insight into the forces and molecular mechanisms associated with bilayer adhesion and fusion, the surface forces apparatus (SFA) was used for measuring the forces and deformations of interacting supported lipid bilayers. Concerning adhesion, we find that the adhesion between two bilayers can be progressively increased by up to two orders of magnitude if they are stressed to expose more hydrophobic groups. Concerning fusion, we find that the most important force leading to *direct* fusion is the hydrophobic attraction acting between the (exposed) hydrophobic interiors of bilayers; however, the occurrence of fusion is not simply related to the strength of the attractive interbilayer forces but also to the internal bilayer stresses (intrabilayer forces). For all the bilayer systems studied, a single basic fusion mechanism was found in which the bilayers do not "overcome" their short-range repulsive steric-hydration forces. Instead, local bilayer deformations allow these repulsive forces to be "bypassed" via a mechanism that is like a first-order phase transition, with a sudden instability occurring at some critical surface separation. Some very slow relaxation processes were observed for fluid bilayers in adhesive contact, suggestive of constrained lipid diffusion within the contact zone.

The traditional view of the fusion of two amphiphilic layers (e.g., two vesicles) is that the two surfaces first overcome their short-range repulsive electrostatic and/or hydration forces so that they can come into close contact (Chernomordic et al., 1987; Westerhoff, 1985; Rand & Parsegian, 1986). However, the relation between interbilayer forces, adhesion, and fusion is still far from clear. There are examples of fusion being induced without apparently altering the interbilayer forces simply by stressing bilayers or by creating an osmotic gradient across them (Chernomordic et al., 1987; Papahadjopoulos et al., 1977; Cohen et al., 1980, 1982; Akabas et al., 1984a,b;

† We thank the National Science Foundation for supporting this work under Grant No. CBT87-21741. Christiane Helm is grateful to the Deutsche Forschungsgemeinschaft for a postdoctoral research scholarship.
* Author to whom correspondence should be addressed.
‡ Johannes Gutenberg-Universität.
§ University of California, Santa Barbara.

0006-2960/92/0431-1794$03.00/0

Ohki, 1982).

Several models of fusion have been suggested, often involving intermediate nonbilayer structures, based on electron micrographs of small vesicles or membranes (Chernomordic et al., 1987; Verkleij et al., 1979a,b, 1984; Miller, 1980; Rand & Parsegian, 1986; Hui et al., 1981; Bearer et al., 1983). The main problem with such experiments is that since fusion normally occurs locally and rapidly (0.1–1 ms), it has been found very difficult to trap the various stages of fusion using conventional freeze–fracture electron microscopy (Chernomordic et al., 1987; Heuser & Reese, 1980; Ornbergh & Reese, 1981). Other proposed models, such as the "stalk" model, have been based on optical visualization and capacitance/conductance measurements of BLM's[1] (Markin et al., 1984; Chernomordic et al., 1987; Leikin et al., 1987; Horn, 1984). The stalk model involves the stochastic exposure of a small hydrophobic group from within the membrane which protrudes from the surface as a "stalk", leading to fusion. Unfortunately, the optical resolution of BLM measurements is too macroscopic to observe such submicroscopic and molecular-scale processes directly. Earlier work on Ca^{2+}-mediated fusion (Ohki, 1982) also suggested that the occurrence of fusion is due to an increased hydrophobicity arising from the condensation of headgroups.

With the aim of shedding more light on some of these questions, we present results of force measurements between adsorbed bilayers in aqueous electrolyte solutions using the SFA technique. The experiments were designed to test the effects of various forces, bilayer fluidity, and homogeneity on interbilayer adhesion, deformation, and fusion, including the time dependence of these processes. A preliminary short report of some of the findings were published by Helm et al. (1989), and for full details of the experimental techniques see Helm and Israelachvili (1992).

Materials and Methods

Materials. Two types of surfactants were chosen for the present study: uncharged zwitterionic double-chain lipids (DMPC, DLPC and egg PC) and the positively charged single-chained surfactant CTAB. The phospholipids were from Sigma (St. Louis, MO) or Avanti (Birmingham, AL), no differences were found between the lipids from these two suppliers. The CTAB from Sigma was recrystallized in 9:1 ethanol/ether. The salt NaBr from Mallinckrodt (Paris, KY) was analytical grade. Water was distilled and additionally filtered in a Labconco purification unit. For the DMPC measurements, the water was first filtered in a Milli-Q unit and subsequently distilled.

Preparation of Supported Bilayers. Both lecithins and CTAB can adsorb from aqueous solution to form "self-assembled" bilayers on mica (surface area of mica used: 1–2 cm^2). CTAB, with its high CMC of 0.8 mM, was always adsorbed from solution as previously described (Israelachvili & Pashley, 1982, 1984; Pashley et al., 1985; Claesson et al., 1986; Kékicheff et al., 1989), and egg lecithin bilayers were adsorbed from a vesicle solution (Horn, 1984). Lecithins are quite insoluble, with CMC's between 10^{-6} and 10^{-10} M (the CMC is normally the critical micelle concentration, but for lipids it is understood to be the critical aggregate or vesicle concentration). Therefore, lipid bilayers were also prepared by the LB technique (with a DPPE monolayer deposited at 40 $Å^2$ with 1.5 cm/min as the first monolayer adjacent to mica), which gives asymmetric bilayers (Marra & Israelachvili, 1985; Marra, 1985, 1986a–c; Israelachvili & Marra, 1986; Helm et al., 1989; Helm & Israelachvili, 1992).

Once bilayers were adsorbed or deposited, forces and interactions were measured and the fringes recorded as described further below. The temperature of the solution was varied and controlled to within 0.3 °C from about 10 to 35 °C by heating or cooling the whole room. An important feature of the present experiments was the progressive dilution of the SFA chamber (volume ~350 mL) with pure water, thereby reducing the concentration of the surfactant solution (the "reservoir") below the CMC and in this way enabling the lipid density in the supported bilayers to be controlled. The chamber has air-tight teflon seals which are opened only to change the solution. When the seals are opened, filters are always there to prevent dust from polluting the chamber.

At the end of an experiment, the apparatus was slowly dried, which removes the outer monolayer and leaves the first hydrophobic layer exposed. This procedure allows the determination of the thickness of the outer monolayer (Marra, 1986a). It is noteworthy that the mica adjacent monolayer did not desorb or appear to be affected by the outer monolayer, at least during the time course of the experiments.

Force Measurements between Undeformed Surfaces. In these experiments the well-established SFA technique was used. This technique allows the measurement of the force laws between two molecularly smooth surfaces (Israelachvili & Adams, 1978; Israelachvili & McGuiggan, 1988; Helm & Israelachvili, 1992). The distance resolution is about 1–2 Å, which is achieved with an optical interference technique using "fringes of equal chromatic order" or FECO. In addition, the deformations parallel to the surfaces can be observed in real time with a lateral distance resolution of about 1 μm.

The force F between two cylindrically curved surfaces of geometric mean radius R is obtained as a function of their separation D from the deflection of a spring. From the measured force, one can obtain the corresponding interaction free energy $W(D)$ per unit area between two flat surfaces as a function of distance D via the Derjaguin approximation (Israelachvili, 1985, 1991):

$$W(D) = F(D)/2\pi R \quad (1)$$

Pressure Measurements between Deformed Surfaces. When two bilayers supported on curved elastic surfaces approach each other, the way they deform on contact (flatten, mainly) depends on the external force pressing them together and on whether the force between them is repulsive or attractive. The different deformations associated with repulsive and attractive forces are reflected in the different FECO fringe patterns they give rise to. These are shown in Figure 1A,B and correspond to local contact geometries shown schematically in Figure 2A,B. Both the contact radius a and surface geometry around a contact zone can be measured from the shapes of the fringes (Helm et al., 1989). Further, dividing the applied force F by the contact area πa^2 gives the mean pressure between the surfaces:

$$P_{mean} = F/(\pi a^2) \quad (2)$$

In the simplest case of two nonadhering surfaces, the surfaces flatten only when an external force is applied, as shown

[1] Abbreviations: BLM, black (or bilayer) lipid membrane; CTAB, hexadecyltrimethylammonium bromide; D_{lat}, lateral diffusion coefficient; DOA, dioctodecyldimethylammonium bromide ($DHDDA^+Br^-$); DGDG, plant digalactosyldiglyceride lipids; MGDG, plant monogalactosyldiglyceride lipids; DLPC, L-α-dilauroylphosphatidylcholine; DMPC, L-α-dimyristoylphosphatidylcholine; DPPC, L-α-dipalmitoylphosphatidylcholine; egg PC, egg yolk phosphatidylcholine; DPPE, L-α-dipalmitoylphosphatidylethanolamine; PC, phosphatidylcholine; PE, phosphatidylethanolamine; PG, phosphatidylglycerol; PS, phosphatidylserine; SFA, surface forces apparatus; LB, Langmuir–Blodgett.

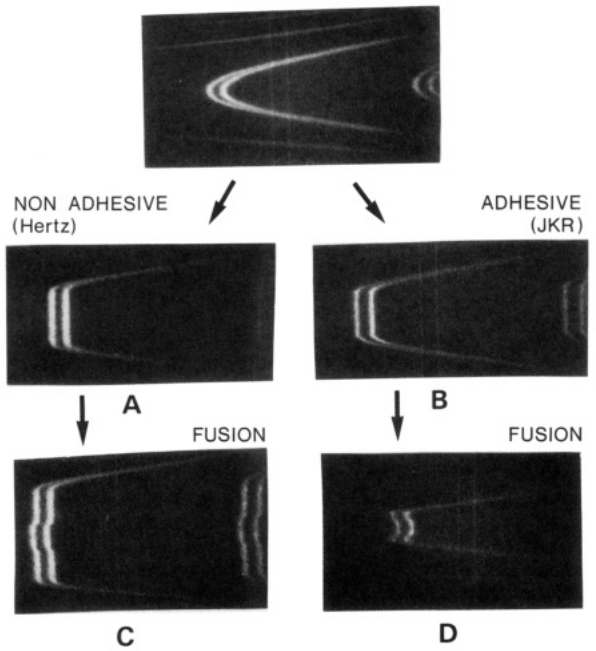

FIGURE 1: Characteristic optical fringe patterns of two supported bilayers. The shapes of these FECO fringes (ignoring the doublets, which are due to the birefringence of the mica) give the cross-sectional profile of the surfaces after noting that the horizontal magnification is 10^4 times higher than the vertical (lateral) magnification. (Top) Curved surfaces not in contact. (A) Bilayers such as DMPC exhibiting little or no adhesion; when pressed together, they deform to give a flattened contact area with rounded corners indicative of smooth bifurcation at the edges. (B) Bilayers exhibiting strong adhesion (like CTAB). The attractive force gives rise to sharper corners indicative of a more abrupt bifurcation at the edges. (C) Hemifusion of weakly adhering bilayers as in panel A usually starts at the center of the contact zone. (D) Hemifusion of strongly adhering bilayers as in panel B often starts at the edges.

in Figures 1A and 2A. The flattened contact radius a then varies with the applied force F according to the "Hertz" theory (Hertz, 1881; Horn et al., 1987):

$$a = (RF/Y)^{1/3} \tag{3}$$

where Y is the elastic modulus of the materials. Further, for Hertzian contacts the pressure P is at a maximum in the center of the contact area, where it is given by $P_{max} = 1.5P_{mean}$, and P decreases monotonically to zero at the edges. As predicted theoretically and shown in Figure 1A, two nonadhering surfaces bifurcate smoothly at the periphery of the contact zone.

Figures 1B and 2B show the very different type of deformations associated with adhesive contacts. Here, the interfacial energy γ, which by definition is half of the adhesion energy W, can be determined from the adhesion or "pull-off" force, F_o, needed to pull the surfaces apart by

$$\gamma = (1/2)W_o = \frac{F_o}{3\pi R} \tag{4}$$

This formula is a result of the Johnson–Kendall–Roberts (JKR) theory (Johnson et al., 1971). The JKR theory predicts that two adhering surfaces bifurcate sharply at the edge of the contact zone, as illustrated in Figures 1B and 2B. The JKR theory is considered to be the basic theory for analyzing the "contact mechanics" or "adhesion mechanics" of adhering surfaces, and it has been well verified experimentally (Johnson et al., 1971; Horn et al., 1987; Chen et al., 1991a).

One interesting feature is sometimes observed that is not predicted by the JKR or other theories of contact mechanics: when the shapes of the FECO fringes are carefully analyzed,

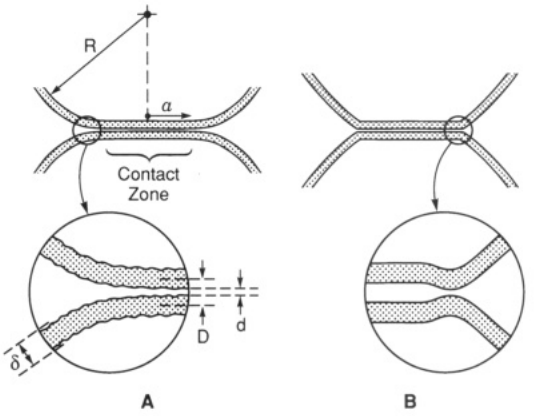

FIGURE 2: Elastic deformations of two mica sheets with a lipid bilayer deposited on each surface as they approach each other in water, as ascertained from the shapes of the FECO fringes (cf. Figure 1). (A) Repulsive (nonadhesive) contacts, schematic illustration of flattened surface profiles when the forces are repulsive. The point of closest approach is at the center of the contact zone, and at the boundary the surfaces bifurcate smoothly. (B) Adhesive contacts: more flattened surface profiles with sharper bifurcation at the boundary of the contact zone. When two surfaces come into adhesive contact, the flattening occurs spontaneously, and the point of closest approach may be at the boundary, which is also the most highly stressed region (Johnson et al., 1971). This figure also defines R (undeformed radius of surfaces), a (radius of contact zone), D (measured distance between bilayer centers across water of two interacting bilayers, where D_o is the equilibrium separation and where $D = 0$ corresponds to "monolayer" contact), d (mean interbilayer separation across water), and δ (hydrated or unhydrated bilayer thickness, where $D = D_0 - \delta_0$ for fully developed noninteracting bilayers and where $D(<D_0) = \delta(<\delta_0)$ for two interacting bilayers). In our experiments, typical values were R = 1 cm, a = 10–100 μm, d = 0.5–2.0 nm, and δ = 3.2–5.9 nm.

it is often apparent that just at the point of bifurcation the two surfaces come *closer in* than in the rest of the contact area (see the circular inset for Figure 2B). As will be discussed later, this highly localized deformation may have important implications for the way adhering bilayers fuse.

RESULTS

Bilayer Deformations during Fusion: the Basic Fusion Mechanism. We first describe the observed fusion mechanisms of two supported bilayers without at this stage considering the types of forces that lead to fusion. One of the most interesting findings was that the deformations associated with the various stages of bilayer fusion are basically the same regardless of the type of headgroup or the number of chains of the constituent lipids. We shall refer to this as the "basic fusion mechanism".

Figure 3 is a schematic of the changing fringe pattern (left side) and corresponding molecular-scale deformations (right side) associated with the basic fusion mechanism. For adsorbed bilayers, fusion always started as "hemifusion" of two bilayers into one bilayer, shown by steps a–e in Figure 3. This is essentially the same as found by Horn (1984) for the fusion of egg PC bilayers, though the first critical "breakthrough" step which triggers the first stage of fusion is here shown in more detail in the inset of Figure 3c. This crucial first breakthrough step starts by a lateral parting of the headgroups on opposite sides of the bilayers, thereby exposing ("opening up") hydrophobic hydrocarbon regions that had been shielded from the aqueous phase in the unstressed bilayers. Due to the long-range nature of the hydrophobic interaction (Israelachvili & Pashley, 1982, 1984; Pashley et al., 1985; Claesson et al., 1986; Christenson & Claesson, 1988; Christenson et al., 1989, 1990; Christenson, 1990; or see Figure 7), these opposing

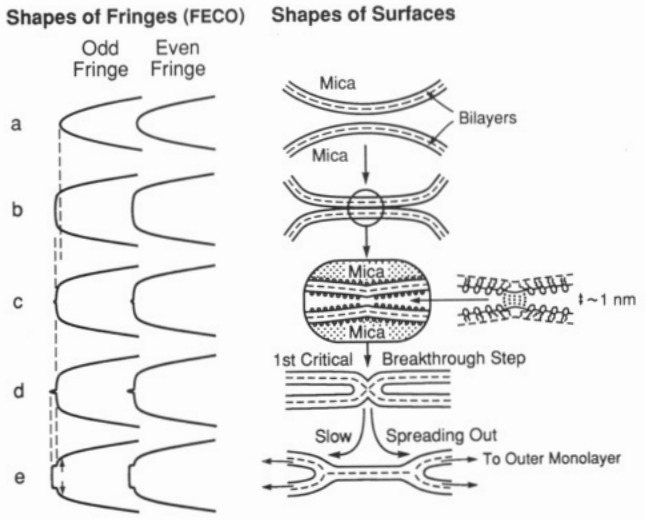

FIGURE 3: Intermediate stages in hemifusion of two adsorbed (supported) bilayers on mica in aqueous solutions (right column) as monitored from the shapes of the FECO fringes (left column). The critical breakthrough step c is followed by sliding out of the lipids from the fused outer monolayers until a single hemifused bilayer remains at step e.

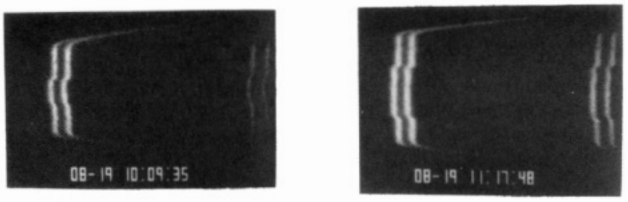

FIGURE 4: Fringe patterns showing a slowly growing hemifused region of two DMPC bilayers in the frozen state. Compared to the very rapid spreading out of the fused region when the bilayers are in the fluid state (Helm et al., 1989), in the frozen state the lipids are extremely immobile, and even after 1 h the fused area does not extend more than a few tens of microns.

hydrophobic regions spontaneously jump together across the gap and fuse. The two outer monolayers of the locally hemifused bilayers now slide radially outward from the fusion site until only one bilayer remains. That hemifusion, rather than full fusion, has taken place could be ascertained from the thickness decrease of the fused region, which corresponded to the thickness of one compressed bilayer, for example, ΔD = 3.4 ± 0.2 nm for fluid DMPC.

Fusion was generally accompanied by a change in the deformed shapes of the adhering surfaces from Hertz-like (Figure 2A) to JKR-like (Figure 2B). This indicates that the adhesion increases during the fusion process, and indeed, on reversing the applied force after hemifusion was complete, a much higher pull-off force was needed to separate the two hemifused monolayers compared to the initial weak adhesion of the unfused bilayers.

The basic hemifusion mechanism described above appears to be quite general for all the surfactant and lipid bilayers we have studied, except that for depleted CTAB bilayers fusion occurred at the edge or boundary of the contact zone rather than at the center, as shown in Figure 1D. Another feature of the basic fusion mechanism is the rate at which the hemifused region spreads out. This is always rapid for bilayers in the fluid state, where tens of microns are traversed in the first second (Helm et al., 1989), but is very slow or nonexistent for bilayers in the gel or frozen state, where the same area was covered in about 1 h (Figure 4).

Role of Intrabilayer Forces on Fusion: Effects of Bilayer Fluidity and Defects. We have found that bilayers composed

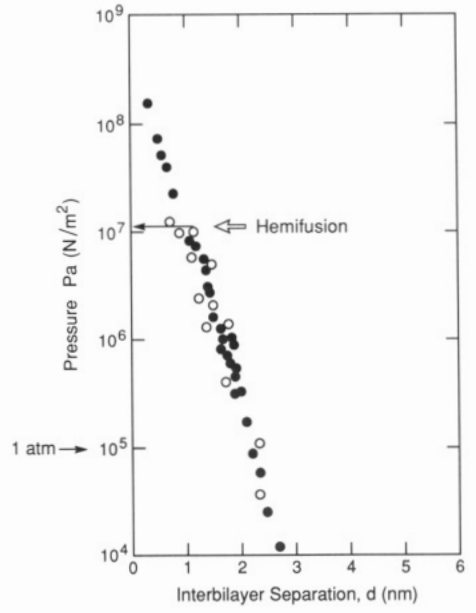

FIGURE 5: Repulsive steric-hydration pressure between two adsorbed egg yolk PC bilayers in saturated vesicle solution at 22 °C as measured using the SFA technique (○), and the osmotic pressure technique (●) by Rand and Parsegian (1989). The forces measured by the two techniques are the same up to at $D \approx 1.2$ nm, where fusion occurred spontaneously between the adsorbed bilayers as shown in Figure 3. Note that since the compressibilities of the monolayers and bilayers were neglected in obtaining these plots, the relative values of D of the two measuring techniques are uncertain by up to 0.4 nm.) In a number of different experiments with bilayers of egg PC from three different batches, fusion generally occurred at pressures ranging from 50 to 110 atm, while with one sample no fusion occurred at the highest pressure attained (about 150 atm).

of pure lipids do not fuse if the bilayers are "fully developed" and "unstressed", that is, so long as the bilayers are in equilibrium with a solution containing lipid/surfactant monomers above the CMC, which acts as a saturated reservoir for the lipids to exchange with. The absence of fusion between unstressed bilayers was noted for pure CTAB, DLPC, and DMPC, the latter both above and below T_c, and up to compressive pressures exceeding 100 atm.

Fusion could be induced by stressing the bilayers. These stresses could be applied in two ways: (i) introducing other components into the bilayers, thereby causing stresses due to packing mismatches and local defects, and (ii) stretching pure bilayers in the fluid state by removing or "depleting" lipids from them. In this section, we describe our results with the first of these stress-inducing mechanisms.

Figure 5 shows results obtained for the repulsive forces between two adsorbed egg lecithin bilayers. For comparison, the results obtained using the osmotic pressure technique on egg lecithin multilayers are also shown. While the forces measured by the two techniques are very similar (Horn et al., 1988), fusion was only observed with the adsorbed bilayers using the SFA technique.

The nature of the osmotic pressure technique, where measurements are carried out across an essentially infinite array of stacked bilayers, hinders the observation of fusion. Moreover, with this technique, as the bilayers approach each other, the molecular area decreases, that is, the bilayers *thicken* (LeNeveu et al., 1976, 1977; Rand & Parsegian, 1989; McIntosh et al., 1988, 1989). The bilayers thus tighten up, thereby making fusion more difficult. In contrast, with the SFA technique, two localized regions of two extended bilayers immersed in water are pressed together. Thus, the change in molecular area will be an increase, that is, the bilayers *thin*,

thereby facilitating their fusion.

In our experiments with egg PC, shown in Figure 5, the adsorbed bilayers would hemifuse spontaneously at some point along the force curve. It is quite remarkable that the critical breakthrough step (Figure 3c) commenced when the bilayers were still about 1.2 nm apart and that up to the point where fusion occurred there was no change in the force curve, i.e., no indication that a dramatic change was about to happen. Actually, the exact pressure where fusion occurred (shown by the arrow in Figure 5) varied with the different sources of egg PC used (note that egg PC is a heterogeneous mixture of different lecithins) and also within the same experiment. This indicates that small defects, probably due to the mixing of different lecithins, eased the breakthrough step. In one experiment with egg PC, *n*-hexane was injected into the aqueous bathing medium, some of which presumably found its way into the bilayers by diffusion (Gruen & Haydon, 1980). Fusion now occurred at an even lower pressure (at about 15 atm compared to 100 as in Figure 5) and from significantly farther out (from D = 1.8 nm compared to 1.2 nm).

The important role of other components was clearly demonstrated when the results with egg PC are compared with those of pure one-component lecithin bilayers (Marra & Israelachvili, 1985; Marra, 1985, 1986a–c; Israelachvili & Marra, 1986; see also Figure 7 below). The forces were very similar to those between egg PC bilayers (Figure 5), but no fusion was ever observed between pure PC bilayers in the fluid state.

Similar observations were made with single-chained fluid bilayers of CTAB adsorbed from bulk solutions around the CMC (~1 mM) corresponding to almost fully developed bilayers. Up to 1–2 h after the surfactant solution was injected into the SFA chamber, both the bilayer thickness and the forces between the bilayers had reached equilibrium, but the bilayers still fused quite easily. However, 24 h later it was not possible to induce fusion, even on applying extremely high pressures. It is likely that after 2 h the adsorption process is still incomplete (Chen et al., 1992) and the bilayers still have tiny defects which serve as fusion sites. With time, these defects anneal out as the bilayers approach their equilibrium unstressed state.

Sometimes, even with pure PC bilayers in the fluid state, certain spots within the contact zone repeatedly acted as sites for fusion. Here, too, it is most likely that some impurity particle, whose lateral dimension was undetectable by our optical technique, had become incorporated into a bilayer and acted as a "fusogen" or "fusogenic site". Actually, creating defects turned out to be the only way to induce hemifusion between DMPC bilayers in the *frozen* state (Figure 4). Such bilayers were prepared by depositing a DMPC monolayer in the fluid state ($T > T_c$) and then cooling below T_c. The induced decrease of molecular area during crystallization apparently caused an uneven coverage. Between such frozen bilayers, the fusion site was always at the same spot or spots, which were not necessarily at the center or edge of the contact zone. This almost certainly indicates that the frozen bilayer was locally damaged (Poste & Allison, 1973; Papahadjopoulos et al., 1973, 1974; Prives & Shinitzky, 1977).

Role of Interbilayer Forces on Fusion. The previous section described how fusion can be induced even when the forces between two bilayers appear to be largely unaffected. We now describe our results where fusion was brought about by specifically altering the interbilayer forces.

The magnitude and range of the attraction between neutral unstressed bilayers, such as lecithin, MGDG, or DGDG, is

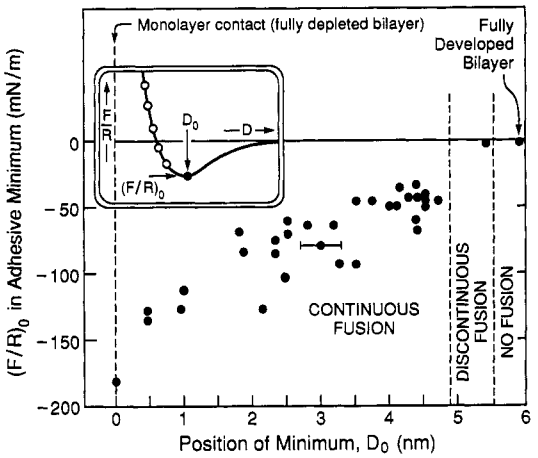

FIGURE 6: Induction of fusion between two Langmuir–Blodgett deposited DMPC monolayers (each on a solid DPPE monolayer, T = 32 °C) by increasing the hydrophobic attraction between them via depletion of the deposited (outer) layer. A schematic drawing of the force law is shown in the inset (see also Figure 7). $D_0 = 0$ corresponds to complete hemifusion (i.e., monolayer contact), whereas the maximum value of D_0 = 5.9 nm corresponds to fully developed bilayers. Note that since D_0 is measured to the potential minimum, it includes the sum of the attractive van der Waals and repulsive steric-hydration forces, i.e., it is the hydrated bilayer thickness. (The error bar shows the typical error in the distance measurements).

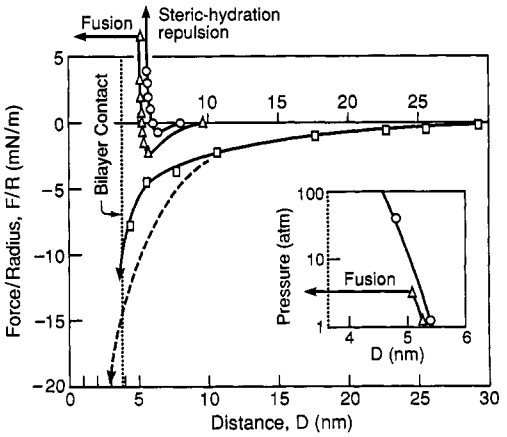

FIGURE 7: Comparison of the force law between PC bilayers in various states of depletion. (○) Forces between two fully developed DMPC bilayer in water saturated with DMPC monomers at 32 °C ($T > T_c$). The attractive van der Waals force causes the two surfaces to jump in from the outermost ○ point, the adhesive minimum being at a bilayer separation of about 2.5 nm. Closer in the steric-hydration repulsion dominates (see inset). (△) Forces between two depleted DLPC bilayers in a partially saturated solution where the bilayers had thinned by 0.5 nm [partly adapted from Marra and Israelachvili (1985)]. The two surfaces now experience a much larger jump into contact from the outermost △ point. (□) Strong hydrophobic attraction between even more depleted DMPC bilayers which spontaneously fuse into one bilayer on jumping into contact. (---) Hydrophobic force between two fully hydrophobic monolayers, according to Christenson and Claesson (1988). (Inset) At high values of F/R, the surfaces flatten elastically where the mean pressure, $P = F/\text{area}$, is a more appropriate measure. The depleted bilayers now fuse at $P \approx 3$ atm, starting in the center. As in the main figure, the dotted line marks the contact of two fully developed anhydrous bilayers.

reasonably well accounted for by the Lifshitz theory of attractive van der Waals forces, especially if the headgroup contribution is included in the computation (Marra & Israelachvili, 1985; Marra, 1985, 1986a–c; Israelachvili & Marra, 1986). This indicates that for fully developed unstressed bilayers in water their hydrophobic regions are effectively shielded from the aqueous phase. But between lipid-depleted DLPC bilayers Marra and Israelachvili (1985) first noted that

both the range and magnitude of the attractive forces increased and that fusion occurred.

Figure 6 shows our results for the increased adhesion force between two fluid DMPC bilayers in contact as a function of decreasing bilayer thickness. Figure 7 shows how, at the same time, the magnitude and range of the long-range attractive forces between the thinned bilayers also increases [see also Helm and Israelachvili (1992)]. Both the enhanced range and magnitude of the attractive forces between these lipid-depleted bilayers cannot be attributed to conventional van der Waals forces and must therefore reflect the additional hydrophobic attraction originating from the newly exposed hydrocarbon groups of the thinned bilayers.

There are at least three ways to thin, or deplete, a bilayer adsorbed on a surface: (i) by depositing a less than fully developed bilayer using the LB technique, (ii) by depleting an initially full bilayer via removal of its lipids, and (iii) by squeezing or stretching a bilayer. In the case of DMPC bilayers, method (ii) was employed whereby the bathing medium was diluted of lipids below the CMC of 5×10^{-8} M (Cevc & Marsh, 1987). Since the lipids in the bilayer and those in the bulk solution are in thermodynamic equilibrium with each other, the reduced monomer concentration induced the LB-deposited bilayer to thin (this was also the way the bilayer thickness was reduced in Figure 6).

If one now allows two such depleted bilayers to slowly approach each other, at some point they jump into adhesive "contact" at $D = D_0$ (Figure 6). The adhesion of the depleted bilayers increases as the bilayer thickness decreases (decreasing D_0), as shown in Figure 6. We have found that once in contact the lipids of the outer monolayers slowly diffuse out of the contact zone, and the bilayers thin further with time. This means that their adhesion also increases the longer they remain in contact. Many of the points in Figure 6 were measured by simply varying the time the bilayers were allowed to remain in contact (for periods up to 1 min) before being separated. In the case of much longer contact times, complete fusion occurred. These time-dependent effects, which were also seen with CTAB bilayers, are described in more quantitative detail later.

The adhesion and fusion results with CTAB are qualitatively similar to those observed with the lecithins. Due to the relatively high solubility of CTAB, the bilayers were invariably adsorbed onto the mica surfaces from a micellar solution. When adsorbed from solutions above the CMC (1 mM and above), the bilayers are fully developed and neither adhesion nor fusion was observed between two such bilayers. As the CTAB concentration is progressively decreased below the CMC, an attractive force developed which resulted in an adhesion force at bilayer–bilayer contact. The adhesion increased as the bilayers became more depleted (Helm et al., 1989) and also with the time the bilayers were allowed to remain in contact before being separated. In addition, the adhesion increased if the bilayers were pressed together while in contact and also if the two surfaces had recently been in contact. Thus, after a separation, two CTAB bilayers had to be kept apart for 5–15 minutes before being brought together again for the adhesion to return to its initial, lower, value.

Hemifusion of two CTAB bilayers could be induced once the bulk solution concentration fell below half the CMC, viz., below about 0.4 mM CTAB (Helm et al., 1989). Eventually, at very low CTAB concentrations (e.g., below 0.2 mM), fusion occurred spontaneously with the bilayers jumping together from the force maximum and fusing straight away into one bilayer without any apparent repulsive barrier.

While CTAB and PC bilayers behave similarly, the sites where fusion occurred within the contact zone were different. With CTAB bilayers, fusion started at the boundary or edge of the circular contact zone rather than at the center, as illustrated in Figure 1B–D. Now, one difference between the two bilayer systems is in the way their force laws vary with separation. Because CTAB is charged, the short-range attractive regime quickly becomes repulsive once $D > 4$ nm (Helm et al., 1989); this causes big deformational stresses at the bifurcating edges which come closer in than the central region (Figures 1B and 2B). In contrast, the attractive force between the uncharged lecithin bilayers was always longer ranged and smoother (Figure 7), resulting in a smoother and more rounded Hertz-like bifurcation where the point of closest approach is at the center rather than at the edges. It is probably for this reason that lecithin bilayers generally fused at the center (Figure 1C) whereas CTAB bilayers fused at the edges (Figure 1D).

Slow Molecular Diffusion in Adhesive Junctions. An unexpected finding was that the interactions between both lecithin and CTAB bilayers in the fluid state were both time- and history-dependent, suggestive of some very slow molecular diffusion or relaxation processes. Time-dependent effects manifested themselves only for depleted bilayers where, after allowing two bilayers to jump into adhesive contact and then keeping them there under no external force, the bilayers progressively thinned and the adhesion increased as a function of time.

Figure 8A shows results for DMPC bilayers initially depleted by about 15% (i.e., 15% thinner than fully developed bilayers). Their progressive thinning and increased adhesion with time (shown in Figure 6) leads to hemifusion after about 5 min in contact. Such bilayers may be thought of as fusing very slowly, in contrast to fully developed bilayers that do not fuse at all or to more depleted bilayers that fuse instantaneously. The bilayers shown in Figure 8A were very depleted (a 15% reduction in thickness is considered large), and only a slight "push" was needed to make them fuse at once. Once the bilayers were brought out of their fused contact, they needed up to 1 h to regain equilibrium, when the adhesion and thinning experiments could be quantitatively reproduced. Otherwise, hemifusion occurred faster or more easily.

An increase of adhesion with time was also observed with CTAB bilayers (Figure 8B), though with CTAB a shorter waiting time of ~10 min was required after each separation to obtain reproducible results. Figures 8 and 9B also show that the adhesion energy of two CTAB bilayers is more or less constant with time during some initial "lag" or "latency" period, after which it increases with time. The adhesion force during the initial lag period was typically $F_0/R \approx 1$ mN/m, which we may note is typical for van der Waals attraction. As might be expected, the lag time was shorter and the rate of adhesion increase faster at lower monomer concentrations, and at 0.2 mM CTAB (about one-fifth of the CMC) fusion occurred instantaneously.

Discussion and Analysis

The Roles of Different Forces in Adhesion and Fusion. We have found that while increasing the attractive or decreasing the repulsive component of the total interaction between two bilayers will always lead to increased adhesion, whether it also favors fusion depends on the origin of the attraction. In particular, we and others (Marra, 1986a,b) find that the existence of a strongly attractive van der Waals or electrostatic force is not sufficient to promote the fusion of bilayers. The reason for this appears to be that these attractive forces act

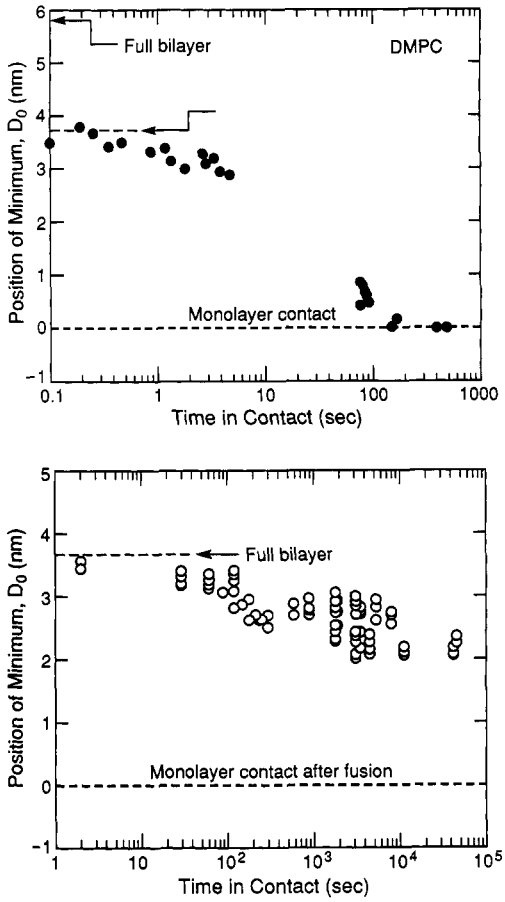

FIGURE 8: Homogeneous thickness decrease of depleted DMPC (top) and CTAB (bottom) bilayers versus time in contact. The bilayers were allowed to jump into contact and then left there while their thickness as a function of time was measured from the fringe positions. (A, top) Thinning of depleted DMPC bilayers in the fluid state (T = 28 °C). The arrow indicates the anhydrous bilayer thickness. Along with the thinning, an increase of the contact area and a sharpening of the bifurcation were observed, indicating increasing adhesion with time. Hemifusion was complete after about 5 min (300 s), when the surfaces came to equilibrium at monolayer–monolayer contact. (B, bottom) Thinning of depleted CTAB bilayers in a solution of 0.5 mM CTAB + NaBr (about half the CMC). In contrast to the DMPC bilayers, complete hemifusion was never attained, and even after 24 h in contact the bilayers still continued to thin (though very slowly).

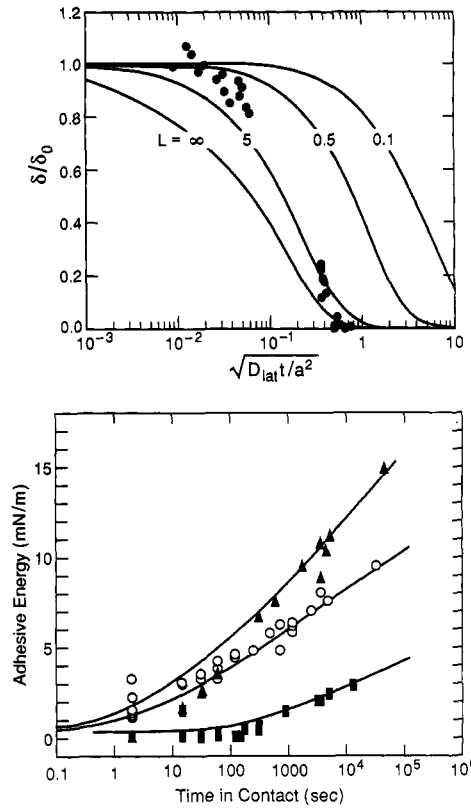

FIGURE 9: (A, top) Relative thickness decrease of the depleted DMPC bilayers shown in Figure 8A (with $\delta_0 \approx 3.8$ nm at $t = 0$) versus normalized time in contact. The lines are numerical solutions of the two-dimensional diffusion equation, as described in the text, for different renormalized boundary permeabilities $L = pa/D_{lat}$, using $D_{lat} = 2 \times 10^{-13}$ m^2/s and the measured radii of contact a, which increased from 8 to 11 μm. (B, bottom) Increase in adhesion energy versus time in contact of CTAB bilayers at the different monomer concentrations below the CMC: 1 mM (■), 0.58 mM (○), and 0.47 mM (▲). The solid lines are the results of numerical calculations using $D_{lat} = 2 \times 10^{-13}$ m^2/s and suitable values for L ($ae^{-45x}/5$ μm for 1 mM, $ae^{-35x}/5$ μm for 0.58 mM, and $ae^{-22x}/5$ μm for 0.47 mM). The adhesive energy was found to be proportional to the relative thinning $x = (\delta_0 - \delta)/\delta$. Note the lag time.

mainly between the outer surface headgroups and not between the interior parts of the membranes. On the other hand, when the membranes are stressed so as to expose hydrophobic groups previously buried within the membranes, the resulting increase in adhesion also leads to fusion.

So far, there has been no satisfactory theory or model for the attractive hydrophobic force, though its long-range exponential distance dependence is now well-established (Israelachvili & Pashley, 1982, 1984; Pashley et al., 1985; Claesson et al., 1986; Christenson & Claesson, 1986, 1988; Christenson et al., 1989, 1990; Kurihara et al., 1990). However, since the hydrophobic force acts between the hydrocarbon interiors of membranes, one can readily understand why it leads to fusion, whereas other types of attractive forces such as Ca^{2+} binding may or may not do so (Papahadjopoulos et al., 1977; Chernomordic et al., 1987; Evans & Metcalfe, 1984; Cohen et al., 1980, 1982; Akabas et al., 1984a,b; Fisher & Parker, 1984; Young et al., 1984, Ohki, 1982; Markin & Kozolov, 1983).

Our results on adhesion and fusion lead to the following scenario: two unstressed bilayers experience a weak initial van der Waals attraction, then, closer in, a much stronger repulsion due to a steric hydration and/or double-layer force (Israelachvili, 1985, 1991; Israelachvili & Wennerström, 1990, 1992). For unstressed bilayers, these forces dominate over the potentially stronger hydrophobic attraction between the hydrocarbon chains. Fusion occurs when bilayers become stressed or stretched so that they locally thin to expose more hydrophobic groups. Such stretching can be achieved in a number of ways depending on whether the bilayers are "free" as in vesicles or "supported" as in our experiments. With adsorbed bilayers, thinning can be achieved by depleting them, by submonolayer deposition, or by pressing them close enough together that the attraction of the locally protruding hydrophobic groups exceeds the headgroup repulsion. This leads to an instability that pulls the hydrocarbon regions of the two bilayers together while pushing the headgroups away (the basic fusion mechanism). This model is actually analogous to a first-order phase transition as occurs during a gas–liquid transition: at large volume (distance) the pressure is repulsive until some nucleation point is reached where there is a sudden collapse in the volume at constant pressure (see horizontal arrows in Figures 5 and 7). In this regard, the basic fusion mechanism is similar to the stalk model (Markin et al., 1984; Chernomordic et al., 1987), but it is also possible that the breakthrough may occur at all once over an extended area rather than at a point as suggested by the stalk model.

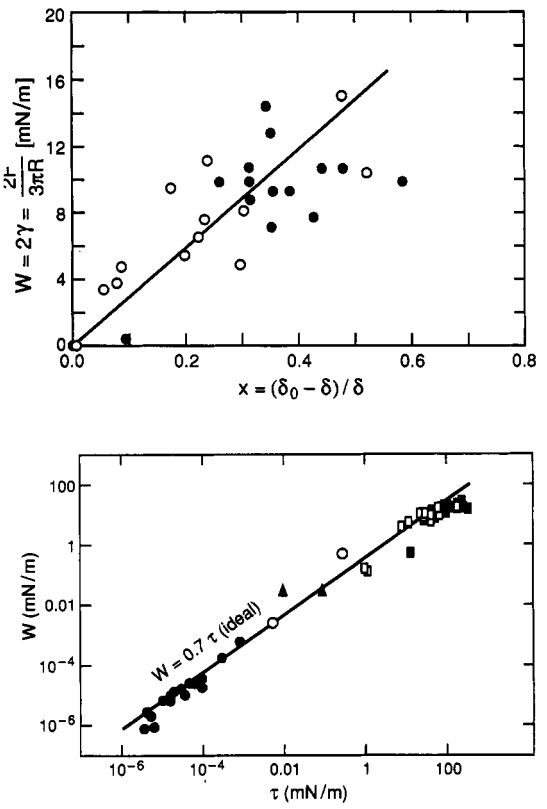

FIGURE 10: (A, top) Measured interfacial energy W versus bilayer thickness decrease x, for both CTAB (○) and DMPC (●). The thicknesses of the fully developed hydrated bilayers were δ_0 = 5.9 nm for DMPC and δ_0 = 3.6 nm for CTAB. (B, bottom) Adhesion energy W versus bilayer tension τ for lecithin bilayers as measured for osmotically swollen bilayers by Servuss and Helfrich (1989) (●), for large vesicles by Evans and Metcalfe (1984) (▲), for small vesicles by Bailey et al. (1990) (○), and for supported DMPC (■) and CTAB (□) bilayers with the SFA technique assuming a bilayer expansion modulus of 150 mN/m. The line is calculated according to eq 8, i.e., $W = 0.7\tau$. Note that both W and τ are plotted on a logarithmic scale.

Relation between Adhesion and Tension of Bilayers. From the data of Figure 6 it appears that the adhesion energy W, defined as twice the interfacial tension γ, increases roughly linearly with decreasing bilayer thickness. For small strains, the experimental data can therefore be expressed as

$$W \approx 2\alpha\frac{(\delta_0 - \delta)}{\delta} \approx 2\alpha x \qquad (5)$$

where δ_0 is the fully developed bilayer thickness and where ideally α should be the value for a purely hydrophobic hydrocarbon–water interface (i.e., $\alpha = \gamma = 50$ mJ/m^2). In Figure 10A, the adhesion energy is shown as a function of the relative thickness decrease $x = (\delta_0 - \delta)/\delta$, both for DMPC and CTAB in the fluid states. In this figure, δ is the thickness of the compressed "bilayer" comprising the two outer fluid monolayers of each adsorbed bilayer (the thickness of the supporting inner monolayers is assumed to be constant). To reduce possible errors inherent in this assumption, only values for small compressions, $x < 0.5$, were taken into account. Then, both sets of data give α = 11–15 mN/m, the range depending on whether W is calculated from the pull-off force F_0 according to $F_0 = (3/2)\pi RW$ or to $F_0 = 2\pi RW$ (Johnson et al., 1971; Derjaguin et al., 1975; Horn et al., 1987). If we assume the molecular volume V to be constant, eq 5 can be written in terms of the molecular area A:

$$W \approx 2\alpha\frac{(V/A_0) - (V/A)}{V/A} \approx 2\alpha\frac{A_0 - A}{A_0} \approx 2\alpha x \qquad (6)$$

Now for free bilayers, changes in area can be brought about by swelling vesicles osmotically (Evans & Metcalfe, 1984; Servuss & Helfrich, 1989), by stretching bilayers hydrostatically (Bailey et al., 1990), by applying an electric field across them (Alvarrez & Latorre, 1978), or by packing stresses from neighboring molecules such as proteins. In many of these cases the bilayer simply expands laterally due to the tension τ generated by these stresses. If K_B is the bilayer expansion modulus, where typically $K_B \approx 150$ mN/m for both free and supported bilayers (Cevc & Marsh, 1987; Evans & Metcalfe, 1984; Chen et al., 1991b), then for small strains the following relation holds:

$$\tau \approx K_B\frac{A_0 - A}{A_0} \qquad (7)$$

which when combined with eq 6 leads to

$$W \approx (2\alpha/K_B)\tau \qquad (8)$$

Thus, our experiments indicate that in a first approximation the adhesion energy W increases linearly with the bilayer tension τ.

A linear dependence between W and τ has previously been measured in independent studies on both osmotically and hydrostatically swollen vesicles. Thus, Figure 10B shows adhesion energies measured by Evans and Metcalfe (1984), Servuss and Helfrich (1989), and Bailey et al. (1990), and those deduced from this and previous studies with the SFA using eq 7. Over a range of over seven orders of magnitude, it is seen that W is indeed roughly proportional to τ with a constant of proportionality of $2\alpha/K_B \approx 0.7$. This may be compared with the "ideal" value expected from eq 8, viz., $2\alpha/K_B = 2\gamma/K_B \approx (2 \times 50)/150 \approx 0.67$. Actually, eq 8 is only approximate and should not be extrapolated too far. Since W cannot exceed $W_{max} \sim 100$ mN/m, at very high tensions the points should deviate from a straight line, as is indeed observed in Figure 10B.

Figure 10B shows remarkably good agreement between a number of very different studies. These include the swelling of large free bilayers and small vesicles (Evans & Metcalfe, 1984; Servuss & Helfrich, 1989; Bailey et al., 1990) and the thinning of supported bilayers using the SFA technique. The first method is suitable for low tensions, while high tensions, up to 100 mN/m, can be achieved only with supported bilayers since free bilayers and vesicles rupture around 3 mN/m.

Our results thus suggest that adhesion and fusion should be enhanced between any laterally stressed bilayers. In free bilayers, such stresses may be induced osmotically, by applying an electric field across two bilayers in close proximity, or via local packing mismatches with other membrane components. There have been many reports that osmotic swelling of vesicles and biological membranes is often necessary for fusion (Chernomordic et al., 1987; Cohen et al., 1980, 1982; Akabas et al., 1984a,b; Fisher & Parker, 1984; Young et al., 1984). Though the popular explanation for this is that the osmotic gradients cause vesicles to rupture and then fuse, we propose that the induction of fusion is more likely to be related to the increased hydrophobicity of the stressed membranes; likewise for electric field-induced fusion, since voltage gradients are known to cause bilayers to thin (Alvarrez & Latorre, 1978). Other fusion-inducing stress mechanisms, including lipid and protein packing stresses, are discussed elsewhere (Helm & Israelachvili, 1992).

Time-Dependent Effects. We have found that both adhesion and fusion are enhanced the longer two laterally stressed fluid bilayers remain in contact and that the bilayers progressively thin with contact time. This suggest that the hydrophobicity

of these bilayers is locally increasing by lateral diffusion of the lipids out of the contact zone. We shall now investigate the energetics and kinetics (time dependence) of this process based on a lateral diffusion model of the lipids out of the contact area.

The outward diffusion of lipid molecules from the outer monolayers of two contacting bilayers results in a thinning of these monolayers. This leads to an increased hydrophobic attraction and thus to a reduction in the total energy of the system. We first analyze the increase in the adhesion energy and final hemifusion of two DMPC bilayers following their jump into contact. The model uses the following assumptions (Crank 1956; Miller & Möhwald, 1987): (i) We assume two-dimensional lateral diffusion of the lipids in the outer monolayers. The crystalline lipids of the supporting inner DPPE monolayers (anchored to the mica) are treated as inert hard walls. They can, however, modify the effective diffusion constant D_{lat} due to the weak interaction between the two monolayers of a bilayer (Seul & McConnell, 1986; Merkel et al., 1989). Any pressure gradients, both lateral or vertical to the bilayers, are assumed not to influence the diffusion behavior. (ii) All deformations of the mica–glue system are described within the framework of the JKR theory (Johnson et al., 1971; Barquins & Maugis, 1982; Horn et al., 1987), which gives for the radius a of the contact circle

$$a^3 = \frac{R}{Y}[F + 6\pi R\gamma + \sqrt{12\pi R\gamma F + (6\pi R\gamma)^2}] \quad (9)$$

where R, F, γ, and Y are defined as before. Note that eq 9 simplifies to eq 3 for $\gamma = 0$. The influence of lateral pressure gradients is neglected.

The calculation basically consists of solving the two-dimensional diffusion equation

$$\frac{\partial c}{\partial t} = D_{lat}\frac{\partial^2 c}{\partial r^2} \quad (10)$$

where c is the two-dimensional lipid concentration, t is the time, and D_{lat} is the lateral diffusion constant. Because of the frictional and compressive forces between the apposing bilayers, the diffusion constant inside the contact zone is likely to be considerable smaller than outside the contact zone. Thus, the diffusion outside the contact zone is going to be neglected in the calculations, and it can be safely assumed that the lipid concentration in the exposed (noninteracting) bilayers is the same everywhere at all times. In mathematical terms, this leads to a so-called evaporation condition rather than to a continuity equation at the boundary or edges (where $r = b$):

$$-D_{lat}\frac{\partial c}{\partial r}\Big|_b = pc_b \quad (11)$$

where p is a boundary permeability coefficient for the molecules to leave the contact area and c_b is the concentration at the boundary. This equation implies that the equilibrium concentration after an infinite time is zero. Using a normalized time scale ($t \rightarrow \sqrt{D_{lat}t}/a$), the diffusion process is a function only of a normalized boundary permeability L (Crank, 1956; Newman, 1931):

$$L = pa/D_{lat} \quad (12)$$

Figure 9A shows the theoretical time dependence of the thinning as calculated according to the conditions outlined above for several values of L. As the figure demonstrates, the theory compares reasonably well with our experimental points for DMPC, which are plotted assuming a lateral diffusion constant of $D_{lat} = 2 \times 10^{-13}$ m^2/s, which is about the lowest value of D_{lat} reported in the literature (Beck, 1987). Since L is not known, one can not determine an unambiguous value for D_{lat}. However, since L cannot exceed ∞, the diffusion constant D_{lat} cannot be lower than the above estimate. Unfortunately, we can say little about the upper limit of D_{lat}. As Figure 9A indicates, for $L \approx 0.5$ the data can also be explained with a value as high as $D_{lat} = 2 \times 10^{-11}$ m^2/s, which is about the highest value reported in the literature (Beck, 1987).

The above analysis shows that the observed long-time relaxation effects of fluid DMPC bilayers can be explained reasonably well in terms of an outward lipid diffusion model using diffusion constants that are similar to previously measured values for monolayers and bilayers. However, more measurements are necessary to fully quantify the diffusion behavior of lipids confined within two interacting bilayers.

As Figures 8 and 9B demonstrate, the outward diffusion of CTAB molecules was much slower than that of DMPC molecules. In addition, the lag times with CTAB were higher than with DMPC. But CTAB bilayers were easier to thin, and their adhesion increased more sharply the more dilute the monomer concentration in the bathing solution. It appears, therefore, that both the L and D_{lat} values for CTAB bilayers are larger than those for DMPC. Possible reasons for this are discussed below.

The logarithmic time dependence of the thinning (Figure 8B) suggests an activation energy-controlled diffusion process of lipid molecules out of the contact zone (with an activation energy barrier at the boundary). They leave the continuously thinning bilayer in the contact area to become part of the less depleted surrounding bilayers, which effectively act as a reservoir. The activation energy at the boundary of the contact zone is likely to increase as the bilayers thin and become more adhesive. To simulate such a diffusion behavior, the method of explicit finite differences was used, as described in the Appendix. As Figure 9B indicates, the model provides a qualitatively correct description of the slowing down of the diffusion process due to the increased adhesion with thinning. As with the DMPC bilayers, L and D_{lat} cannot be determined independently.

We now turn to consider possible reasons for the slower outward diffusion/thinning of CTAB bilayers compared to the DMPC monolayers on DPPE. First, the hydrocarbon chain interdigitation of two fluid CTAB monolayers is greater than that of a fluid DMPC monolayer in contact with a solid crystalline DPPE monolayer (Chen et al., 1991a). This causes a much larger drag on the lateral movement of CTAB molecules than on the DMPC molecules, even though the latter have a larger volume. It is also possible that the sharper bifurcation of the CTAB surfaces at the boundary or edge of the contact zone (cf. Figures 1B and 2B inset) leads to a further reduced boundary permeability of molecules out of the contact zone into the "reservoir".

Comparison of Supported versus Free Bilayers. We cannot say whether the basic mechanism we have observed for our adsorbed or "supported" surfactant and lipid bilayers is the same as occurs between "free" bilayers or membranes in solution, though there is good evidence that vesicles in solution do indeed adhere and fuse by going through the same stages as depicted in Figure 3 (Chernomordic et al., 1987; Hui et al., 1981). In many real cases, the transition from adhesion through monolayer fusion to full fusion may be continuous, going rapidly through the stages of Figure 3 and then rupturing. Such a mechanism is not inconsistent with experimental data on vesicle and membrane fusion. In addition, it is very simple and does not require any complicated intermediate structures such as inverted micellar structures. Our

experiments show that during fusion no such intermediate structures occur *within* the fusion zone, though they may appear at the boundary just outside the fused area, as has previously been reported (Rand & Parsegian, 1986; Verkleij et al., 1979a,b, 1984; Miller, 1980).

It is instructive to estimate the forces and energies involved in the elastic deformation of the supporting elastic surface when hemifusion occurs. As the limiting step, the deformation at the breakthrough is probably the most important. Here we shall attempt to calculate the size of the critical breakthrough area by analyzing the protruding tip or stalk within a continuum framework. We shall adopt the model by Pethica and Sutton (1980) for the elastic deformations that an atomic force microscope (AFM) tip induces on the opposite surface.

For the depleted bilayers, an attractive hydrophobic energy $\Phi(x) = 2\gamma e^{-D\beta}$ per unit area is assumed, where $\gamma = 50$ mN/m is the interfacial tension, D is the distance between the bilayers, and $\beta^{-1} \approx 1.0$ nm is the decay length for the hydrophobic interaction (Israelachvili & Pashley, 1982, 1984; Pashley et al., 1985; Claesson et al., 1986; Christenson & Claesson, 1988; Christenson et al., 1989, 1990; Christenson, 1990). Thus, knowing the attractive force per unit area, $-\partial\Phi/\partial D$, the minimum radius r_{crit} of a strongly depleted spot big enough to induce hemifusion can now be estimated. The model requires us to calculate the elastic deformation energy of the breakthrough region, which is modeled as a cylinder of radius r protruding a distance h from one of the surfaces. Just as a "jump-in" occurs in measurements of attractive forces (Israelachvili & Adams, 1978; Israelachvili & McGuiggan, 1988; Helm & Israelachvili, 1992), an instability and thus a protruding deformation will occur if the surface rigidity $S = \partial\Phi/\partial h$ equals the slope of the force $\partial\Phi/\partial D$. The instability is irreversible if the surface force has a stronger distance dependence than the elastic restoring force S. Everything is now straightforward, using Boussinesq's relation for the deformation due to a point load (Pethica & Sutton, 1980):

$$\partial h = F/\pi\rho E^* \tag{13}$$

where E^* is the the elasticity constant for the composite bilayer–mica–glue system (Pethica & Sutton, 1980; Horn et al., 1987) and ρ is the distance from the center of the tip. Note that after the breakthrough, once hemifusion starts, it will continue to spread since the elastic bending energy is now less than that needed to initiate the instability. Equation 13 gives for h

$$h = \int_0^r 2\pi\rho \frac{\partial\Phi}{\partial D} \frac{1}{\pi E^* \rho} \, d\rho \tag{14}$$

and for the force

$$F = \int_0^r 2\pi\rho \frac{\partial\Phi}{\partial D} d\rho \tag{15}$$

Thus, $S = E^*\pi r/2$ and $\partial F/\partial D = 2\pi r^2\gamma\beta^2 e^{-\beta D}$, so that the slope of the force exceeds the surfaces rigidity only if r is larger than a minimum size given by

$$r_{crit} = E^*/(4\gamma\beta^2) \tag{16}$$

Using $E^* = E/(1 - \nu^2) = 1.5Y$ where $Y = 1.1 \times 10^{10}$ N/m^2, and the numbers given above, we obtain $r_{crit} \approx 37.5$ nm. Assuming an area per lipid molecule of ~ 1 nm^2, this would involve some 4500 molecules in each bilayer participating in the fusion breakthrough.

This number is probably an upper limit, since we always observed fusion to take place at a point in the contact zone, where additional JKR-type stresses caused by the deformations of the support were exerted on the bilayer. Nevertheless, this calculation suggests that the breakthrough spot may be quite extended, supporting the idea of a locally depleted area of contacting bilayers just prior to fusion.

Summary of Main Results

Our four main conclusions are as follows:

Adhesion and Fusion-Promoting Forces. The interbilayer forces that enhance bilayer adhesion do not necessarily promote fusion, and in general the force law between bilayers is no indicator of whether fusion will occur or not. The major force that leads to *direct* bilayer fusion is the hydrophobic attraction between the internal hydrophobic hydrocarbon groups that have become exposed to the aqueous phase. Only a small increase in the exposed hydrocarbon area is required to substantially increase the adhesion energy and facilitate fusion.

Basic Fusion Mechanism. Fusion can be triggered spontaneously between two repelling bilayers when they are still at a finite distance from each other without their having to first overcome the short-range repulsive forces, e.g., the steric hydration barrier. Localized molecular rearrangements allow this to happen by a process of locally bypassing these forces via a simple breakthrough mechanism that does not require any complex nonbilayer intermediate structures and that may apply to other bilayer and biological membrane systems.

Relation between Bilayer Stresses and Fusion. Fusion starts locally at the weakest or most highly stressed point of two apposing bilayers. Depending on the adhesion and the range of the attractive hydrophobic force between the two stressed regions, this can be at the center or the edge of the contact zone or at a locally stressed defect point.

Lipid Diffusion out of the Contact Zone. We have found that the lipids in the contact zone of depleted bilayers can diffuse out of the contact region. This effect is manifested as a decrease in the bilayer thickness accompanied by an increase in the adhesion energy with time, eventually (but not always) leading to fusion. The diffusion is driven by the energy gain due to increased hydrophobic interaction. The actual time dependence is dominated by the barrier between contacting and free bilayers and is well described by a phenomenological diffusion model. The diffusion can be surprisingly slow.

While our findings should be directly applicable to the interactions of surfactant-coated colloidal particles, it is too early to say whether they also apply to the fusion of biological membranes. The latter, in particular, are expected to involve much more specific interactions than we have in our simple system. Nevertheless, there are good reasons why at least the qualitative observations we have made on supported bilayers do appear to apply to the interactions of free bilayers and vesicles interacting in solution.

Acknowledgments

We thank Roger Horn for allowing us to include previously unpublished data (Figure 5) and Evan Evans, Stuart McLaughlin, Helmuth Möhwald, Vladislav Markin, Joe Zasadzinski, Albrecht Weisenhorn, and Jim Hardin for constructive comments.

Appendix

To simulate the diffusion process, the method of explicit finite differences was employed. In addition to the two major assumptions (i) and (ii) given in the text, the following approximations were made:

(iii) The adhesion energy W is simply proportional to the relative thickness decrease x (which is identical to the relative area increase) as described in eq 5 with $\alpha = 15$ mN/m. According to the JKR–Hertz theories, eqs 3 or 9, the radius

a of the contact zone therefore increases with x according to $a \approx 24x^{1/3}$ μm.

(iv) Assuming that the volume of a lipid molecule is not affected by its lateral concentration c (given by $c = 1/A$, where A is the area per molecule), c is then related to x by

$$c = \frac{1}{A} = \frac{1}{A_0(1 + x)} = \frac{c_0}{1 + x} \tag{A1}$$

where c_0 and A_0 are the lateral concentration and the molecular area of a lipid within a fully developed bilayer, respectively.

(v) The boundary permeability coefficient is assumed to contain an activation energy barrier that the lipids have to overcome when they move from the highly depleted contact area into the surrounding free bilayers. Thus

$$p = p_0 e^{-\kappa x} \tag{A2}$$

which leads to a normalized boundary permeability coefficient

$$L = \frac{ap_0}{D_{lat}} e^{-\kappa x} \tag{A3}$$

The boundary permeability coefficient, and thus both p_0 and κ, are bound to be influenced by the deformations of the bilayers and the stresses at the edges, which were determined by numerical simulations.

(vi) x is determined as the average value of the concentration distribution within the contact zone.

The discrete steps in the calculation were as follows: (1) At a fixed time t and given x, the radius of the contact zone a grows until it is bigger than $24x^{1/3}$ μm. (2) Diffusion starts and x increases until the radius a is smaller than $24x^{1/3}$ μm. (3) The growth according to step 1 continues and steps 1 and 2 are reiterated.

The step size was varied between $\Delta r = 2$ nm and a system radius of 1000 nm and a step size of $\Delta r = 10$ nm and a system radius of 5000 nm, depending at which time scale the diffusion should be simulated. c_b, the boundary concentration, was taken to be the one of the surrounding (not contacting) bilayers. With increasing depletion, the activation barrier increases, slowing down the diffusion process more and more. Typical results showing the calculated time dependence of the adhesion energy are given in Figure 9B assuming a diffusion constant of $D_{lat} = 2 \times 10^{-13}$ m^2/s. Since the contact radius a is variable in these simulations, L can be given only as a function of a. Similar to the diffusion with constant boundary permeability, the diffusion constant in these experiments cannot be determined, since the time scales with $1/D_{lat}$. In the same way, the normalized boundary permeability coefficient L, which determines the lag time, scales with $1/D_{lat}$. Thus, assuming a lateral diffusion constant of $D_{lat} = 2 \times 10^{-11}$ m^2/s (the higher limit given in the literature), L would decrease by two orders of magnitude.

Registry No. CTAB, 57-09-0; DLPC, 18194-25-7; DMPC, 63-89-8.

References

Akabas, M. H., Cohen, F. S., & Finkelstein, A. (1984a) *J. Cell Biol. 98*, 1054.

Akabas, M. H., Cohen, F. S., & Finkelstein, A. (1984b) *J. Cell Biol. 98*, 1063.

Alvarrez, O., & Latorre, R. (1978) *Biophys. J. 21*, 1.

Bailey, S. M., Chiruvolu, S., Israelachvili, J. N., & Zasadzinski, J. A. N. (1990) *Langmuir 6*, 1326.

Barquins, M., & Maugis, D. (1982) *J. Mec. Theor. Appl. 1*, 331.

Bearer, E. L., Duzgunes, N., Friend, D. S., & Papahadjopoulos, D. (1983) *Biochim. Biophys. Acta 693*, 93.

Beck, K. (1987) in *Cytomechanics* (Bereiter-Hahn, J., Anderson, O. R., & Reif, W.-E., Eds.) Springer Verlag, Berlin, Heidelberg.

Cevc, G., & Marsh, D. (1987) *Phospholipid Bilayers*, Chapter 2, Wiley, New York.

Chen, Y. L., Helm, C. A., & Israelachvili, J. N. (1991a) *J. Phys. Chem.* (in press).

Chen, Y. L., Helm, C. A., & Israelachvili, J. N. (1991b) *Langmuir 7*, 2694.

Chen, Y. L., Helm, C. A., & Israelachvili, J. N. (1992) *J. Colloid Interface Sci.* (submitted).

Chernomordic, L. V., Melikyan, G. B., & Chizmadzhev, Y. A. (1987) *Biochim. Biophys. Acta 906*, 309.

Christenson, H. K. (1990) in *Modern Approaches to Wettability* (Schnader & Loeb, Eds.) Plenum Press, New York.

Christenson, H. K., & Claesson, P. M. (1988) *Science 239*, 390.

Christenson, H. K., Claesson, P. M., Berg, J., & Herder, P. C. (1989) *J. Phys. Chem. 93*, 1472.

Christenson, H. K., Fang, J., Ninham, B. W., & Parker, J. (1990) *J. Phys. Chem. 94*, 8004.

Claesson, P. M., Blom, C. E., Herder, P. C., & Ninham, B. W. (1986) *J. Colloid Interface Sci. 114*, 234.

Cohen, F. S., Zimmerberg, J., & Finkelstein, A. (1980) *J. Gen. Physiol. 75*, 251.

Cohen, F. S., Akabas, M. H., & Finkelstein, A. (1982) *Science 217*, 458.

Crank, J. (1956) *The Mathematics of Diffusion*, Oxford University Press, Oxford.

Derjaguin, B. V., Muller, V. M., & Toporov, Y. P. (1975) *J. Colloid Interface Sci. 53*, 314.

Evans, E., & Metcalfe, M. (1984) *Biophys. J. 46*, 423.

Fisher, L. R., & Parker, N. S. (1984) *Biophys. J. 46*, 253.

Granfeldt, M. K., & Miklavic, S. J. (1991) *J. Chem. Phys. 95*, 6351.

Gruen, D. W. R., & Haydon, D. A. (1980) *Biophys. J. 30*, 129.

Helm, C. A., & Israelachvili, J. N. (1992) *Methods Enzymol.* (in press).

Helm, C. A., Israelachvili, J. N., & McGuiggan, P. (1989) *Science 246*, 919.

Hertz, H. J. (1881) *Reine Angew. Math. 92*, 156.

Heuser, J. E., & Reese, T. S. (1980) *J. Cell Biol. 88*, 564.

Horn, R. G. (1984) *Biochim. Biophys. Acta 778*, 224.

Horn, R. G., Israelachvili, J. N., & Pribac, F. (1987) *J. Colloid Interface Sci. 115*, 480.

Horn, R. G., Israelachvili, J. N., Marra, J., Parsegian, V. A., & Rand, R. P. (1988) *Biophys. J. 54*, 1185.

Hui, S. W., Stewart, T. P., Boni, L. T., & Yeagle, P. L. (1981) *Science 212*, 921.

Israelachvili, J. N. (1985) *Intermolecular and Surface Forces*, Academic Press, New York; (1991) 2nd ed.

Israelachvili, J. N., & Adams, G. E. (1978) *J. Chem. Soc., Faraday Trans. 1 74*, 975.

Israelachvili, J. N., & Pashley, R. M. (1982) *J. Colloid Interface Sci. 98*, 500.

Israelachvili, J. N., & Pashley, R. M. (1984) *Nature 300*, 341.

Israelachvili, J. N., & Marra, J. (1986) *Methods Enzymol. 127*, 353.

Israelachvili, J. N., & McGuiggan, P. M. (1988) *Science 271*, 795.

Israelachvili, J. N., & Wennerström, H. (1990) *Langmuir 6*, 873.

Israelachvili, J. N., & Wennerström, H. (1992) *J. Phys. Chem.* (in press).

Johnson, K. L., Kendall, K., & Roberts, A. D. (1971) *Proc. R. Soc. London A 324*, 301.
Kékicheff, P., Christenson, H. K., & Ninham, B. W. (1989) *Colloids Surf. 40*, 31.
Kurihara, K., Kato, S., & Kunitake, T. (1990) *Chem. Lett. Chem. Soc. Jpn. 1990*, 1555.
Leikin, S. L., Kozlov, M. M., Chernomordik, L. V., Markin, V. S., & Chizmadzhev, Y. A. (1987) *J. Theor. Biol. 129*, 411–425.
LeNeveu, D. M., Rand, R. P., Parsegian, V. A., & Gingell, D. (1976) *Nature 259*, 601.
LeNeveu, D. M., Rand, R. P., Parsegian, V. A., & Gingell, D. (1977) *Biophys. J. 18*, 209.
Markin, V. S., & Kozlov, M. M. (1983) *Gen. Physiol. Biophys. 2*, 201.
Markin, V. S., Kozlov, M. M., & Borovjagin, V. L. (1984) *Gen. Physiol. Biophys. 5*, 361.
Marra, J. (1985) *J. Colloid Interface Sci. 107*, 446.
Marra, J. (1986a) *Biophys. J. 50*, 815.
Marra, J. (1986b) *J. Phys. Chem. 90*, 2145.
Marra, J. (1986c) *J. Colloid Interface Sci. 109*, 11.
Marra, J., & Israelachvili, J. N. (1985) *Biochemistry 24*, 4608.
McCown, J. T., Evans, E., Diehl, S., & Wiles, H. C. (1981) *Biochemistry 20*, 3134.
McIntosh, T. J., Magid, A. D., & Simon, S. A. (1988) *Biochemistry 26*, 7325.
McIntosh, T. J., Magid, A. D., & Simon, S. A. (1989) *Biochemistry 28*, 7904.
Merkel, R., Sackmann, E., & Evans, E. (1989) *J. Phys. (Paris) 50*, 809.
Miller, A., & Möhwald, H. (1987) *J. Chem. Phys. 85*, 4528.
Miller, R. G. (1980) *Nature 287*, 166.
Newman, A. B. (1931) *Trans. Am. Inst. Chem. Eng. 27*, 203.
Ohki, S. (1982) *Biochim. Biophys. Acta 689*, 1.
Ornbergh, R. L., & Reese, T. S. (1981) *J. Cell Biol. 90*, 40.
Papahadjopoulos, D., Poste, G., & Schaeffer, B. E. (1973) *Biochim. Biophys. Acta 323*, 23.
Papahadjopoulos, D., Poste, G., Schaeffer, B. E., & Vail, W. J. (1974) *Biochim. Biophys. Acta 352*, 10.
Papahadjopoulos, D., Vail, W. J., Newton, C., Nir, S., Jacobson, K., Poste, G., & Lazo, R. (1977) *Biochim. Biophys. Acta 465*, 579.
Pashley, R. M., McGuiggan, P. M., Ninham, B. W., & Evans, D. F. (1985) *Science 229*, 1088.
Pethica, J. B., & Sutton, A. B. (1980) *J. Vac. Sci. Technol., A 6(4)*, 2490.
Poste, G., & Allison, A. C. (1973) *Biochim. Biophys. Acta 300*, 421.
Prives, J., & Shintzky, M. (1977) *Nature 268*, 761.
Rand, R. P., & Parsegian, V. A. (1986) *Annu. Rev. Physiol. 48*, 201.
Rand, R. P., & Parsegian, V. A. (1989) *Biochim. Biophys. Acta 988*, 351.
Servuss, R. M., & Helfrich, W. (1989) *J. Phys. (Paris) 50*, 809.
Seul, M., & McConnell, H. (1986) *J. Phys. (Paris) 47*, 1587–1604.
Verkleij, A. J., Mombers, C., Leunissen-Bijvelt, L., & Ververgaert, P. H. (1979a) *Nature 279*, 162.
Verkleij, A. J., Mombers, C., Gerritsen, W. J., Leunissen-Bijvelt, L. & Cullis, P. R. (1979b) *Biochim. Biophys. Acta 555*, 358.
Verkleij, A. J., Leunissen-Bijvelt, L., De Kruijff, B., Hope, M., & Cullis, P. R. (1984) in *Cell Fusion*, p 355, Pitman Books, London.
Westerhoff, H. V. (1985) *Trends Biochem. Sci. 10*, 134.
Young, T. M., Ding, E., & Young, J. (1984) *Biochim. Biophys. Acta 775*, 441.